Modifying the Ni-MoS_2 Contact Interface Using a Broad-Beam Ion Source

Zhihui Cheng, *Student Member, IEEE*, Jorge A. Cardenas, *Student Member, IEEE*, Felicia McGuire, *Student Member, IEEE*, Sina Najmaei, and Aaron D. Franklin, *Senior Member, IEEE*

***Abstract*— Charge transport at the contacts is a dominant factor in determining the performance of devices using 2D MoS_2. Using a low-energy beam of Ar ions, the interface between Ni and MoS_2 was modified to improve the performance in 2D field-effect transistors (FETs). This broad-beam ion source is integrated into an ultrahigh vacuum, physical vapor deposition system that allowed for *in situ* modification of the MoS_2 immediately prior to Ni contact deposition. The contact resistance decreased leading to a corresponding and highly reproducible boost in the on-current by up to four times. Spectroscopic analysis of the ion beam-modified MoS_2 suggests that there are generated defects, which supply dangling bonds that improve carrier injection between the Ni metal contact and MoS_2. This approach for modifying the Ni-MoS_2 interface opens a promising new path for reducing the impact of contacts on MoS_2 FET performance.**

***Index Terms*— MoS_2, field-effect transistor (FET), contact resistance, ion beam, carrier injection, 2D.**

I. Introduction

Atomically thin, two-dimensional (2D) materials have attracted wide interest for electronic applications in recent years [1]–[8]. While the study of 2D field-effect transistors (FETs) began with graphene [9], its lack of an energy band gap led to a shift in focus on semiconducting 2D materials, such as transition metal dichalcogenides (TMDs) that have a tunable band gap and reasonable mobility [6]–[9]. Most prominent of the various TMDs has been MoS_2, which has the potential to enable scaling of the transistor channel down to sub-5 nm lengths [13]. Since the first MoS_2 FET was demonstrated in 2011 [14], numerous reports have been published related to the FET structure and performance limits. What remains clear is that contact effects are a dominant challenge in realizing the ultimate potential of 2D FETs.

Several techniques have been shown to improve carrier transport at the metal-MoS_2 interface, thus lowering the contact resistance (R_c). These approaches include the use of molecular doping [15], different contact material [16]–[19], phase transformation of MoS_2 [20], and adding an interfacial oxide at the contacts [2], [21]. The challenge of these techniques is that they generally require additional processing, sometimes involving very high temperatures, or the addition of materials at the metal-MoS_2 interface that may lower contact resistance but still yield relatively poor FET performance. For example, in [20] R_c as low as 200 $\Omega \cdot \mu$m was reported with an on-current of only 85 μA/μm (similar to devices with orders of magnitude higher R_c). In graphene, it has been demonstrated that intentionally damaging the crystal lattice in the contact region using O_2 plasma can substantially reduce R_c and boost performance [22]–[24]. In this work, we systematically examine a related contact engineering approach for MoS_2 FETs by using an *in situ*, broad-beam ion source to modify the MoS_2 lattice immediately prior to contact metal deposition. The result is a substantial improvement in device performance.

Manuscript received June 16, 2016; revised July 7, 2016; accepted July 10, 2016. Date of publication July 14, 2016; date of current version August 23, 2016. This work was supported by the National Science Foundation under Grant ECCS 1508573. The review of this letter was arranged by Editor M. Passlack.

Z. Cheng, F. McGuire, S. Najmaei, and A. D. Franklin are with the Department of Electrical and Computer Engineering, Duke University, Durham, NC 27708 USA (e-mail: aaron.franklin@duke.edu).

J. A. Cardenas is with the School of Electrical, Computer, and Energy Engineering, Arizona State University, Tempe, AZ 85287 USA.

Color versions of one or more of the figures in this letter are available online at http://ieeexplore.ieee.org.

Digital Object Identifier 10.1109/LED.2016.2591552

II. Device Fabrication

The process flow for fabricating the back-gated MoS_2 FETs used in this study, illustrated in Fig. 1(a-d), involved first mechanically exfoliating MoS_2 (2D Semiconductors, Inc.) and transferring it to p++ Si wafers with 10 nm SiO_2. The approximate thickness of all MoS_2 flakes used in this study is 7 nm, as verified using atomic force microscope (AFM) imaging. After coating the substrate with poly (methyl methacrylate) (PMMA), electron-beam lithography (EBL) was used to pattern the source/drain contacts. For the baseline FETs without ion beam modification, 25 nm of Ni was then deposited in the contact regions, followed by lift-off in acetone. A second set of FETs was then fabricated on the same MoS_2 flake using EBL to once again form the contact pattern in PMMA. Then, in a custom-designed ultra-high vacuum (UHV) chamber (LAB Line, Kurt J. Lesker Company), the chip was exposed to an Ar ion beam (eH400, KRi) to modify the MoS_2 selectively in the contact regions under a base pressure of 2×10^{-8} torr. A schematic of the setup is shown in Fig. 1(e), where the broad-beam ion source is installed at an angle, incident on the substrate and at a throw distance of 12”. The chamber includes an electron-beam evaporator that allowed for the deposition of 25 nm Ni contacts after ion beam exposure without subjecting the chip to the ambient. After lift-off of the second set of contacts, contact pads (2 nm Ti / 30 nm Pd / 30 nm Au) were formed. Devices were electrically characterized in air.

In order to achieve the most reliable information regarding the impact of the broad-beam ion source on the Ni-MoS_2 interface, two sets of FETs were fabricated on each MoS_2

0741-3106 © 2016 IEEE. Personal use is permitted, but republication/redistribution requires IEEE permission.
See http://www.ieee.org/publications_standards/publications/rights/index.html for more information.

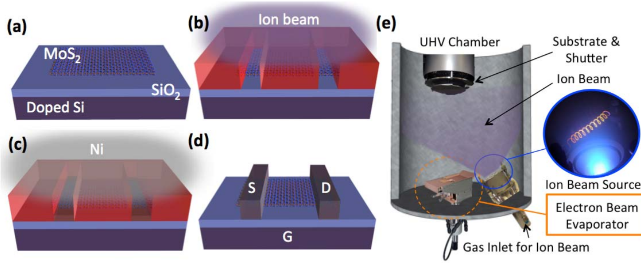

Fig. 1. Fabrication process flow for MoS_2 FET with contact interface modified using a broad-beam ion source. (a) Transfer of MoS_2 onto doped Si chip with 10 nm SiO_2 using mechanical exfoliation. (b) PMMA coating, EBL contact patterning, and selective exposure of MoS_2 in the contact regions to the broad-beam ion source. (c) 25 nm Ni metal deposition immediately after ion beam exposure and without removing sample from UHV. (d) Lift-off in acetone to complete the MoS_2 FET. (e) Schematic of the custom UHV system incorporating both the broad-beam ion source and an electron-beam evaporator for contact metal deposition.

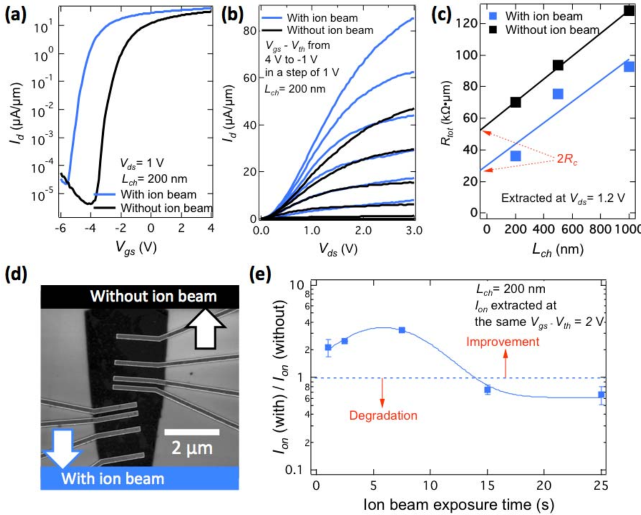

Fig. 2. Electrical characteristics showing impact of Ni-MoS_2 interface modification with a broad-beam ion source. (a) Subthreshold curves of devices with channel lengths of 200 nm on the same MoS_2 flake. Ion beam exposure was at 60 V and 0.5 A for 1 s. (b) Output curves for the same devices as in (a), plotted at the same gate overdrive voltage (V_{gs}–V_{th}) to account for the V_{th} shift. (c) TLM plot of total resistance for the two sets of devices showing extraction of contact resistance. (d) SEM image of the two sets of devices on the same MoS_2 flake. (e) Improvement of on-current versus exposure time, plotted as the ratio of I_{on} with ion beam modification (I_{on} (with)) and I_{on} from the baseline device (I_{on} (without)) from the same flake; each data point is the average from dozens of devices with error bars indicating standard deviation.

flake—one set without exposure to the ion beam and one with exposure. This reduces the large variability that is common for MoS_2 devices built on different flakes, due to variations in thickness and defect density. Dozens of chips were fabricated and studied having different exposure conditions (voltage and time) to the broad-beam ion source. Each chip contained 8-10 MoS_2 flakes with targeted channel lengths for each set of devices of 200 nm, 500 nm and 1 μm, with a width of $\sim$2 μm.

III. Results and Discussion

Characteristics of a representative set of MoS_2 devices are given in Fig. 2. The broad-beam ion source conditions for the modified devices included an exposure time of 1 s, discharge current of 0.5 A, and discharge voltage of 60 V, yielding a current density of $\sim$0.04 mA/cm^2. As can be seen in the subthreshold curves of Fig. 2(a), the subthreshold swing remains essentially unchanged while there is a threshold voltage (V_{th}) shift of -2 V. While some V_{th} shift may be caused by the ion beam modification, a variation in V_{th} of several volts was observed even in baseline devices on the same flake, making it not possible to deduce the precise cause of the shift beyond variation in trapped charge at the MoS_2-SiO_2 interface as discussed in other reports [25].

For the on-state performance, output curves for 200 nm channel devices are shown in Fig. 2(b). The device with the modified Ni-MoS_2 interface exhibits twice the on-current (I_{on}) as the comparable device without ion beam exposure (baseline device) from the same flake and at the same gate overdrive (V_{gs} - V_{th}). If all three different channel length devices in a set worked, then contact resistance could be extracted using the transfer length method (TLM). A plot of the total resistance (R_{tot}), which is the measured resistance multiplied by device width, at $V_{ds} = 1.2$ V versus the channel length (L_{ch}) is shown in Fig. 2(c). The effect of threshold voltage shifts has been accounted for in the calculated R_{tot}. Importantly, the sheet resistance (slope of the linear fit to the TLM data, extracted to be 0.0723 k$\Omega \cdot \mu$m) of the MoS_2 is consistent between the two device sets—a benefit of fabricating the devices on the same flake. Extracted from an extrapolation of the linear fit to the TLM plot, $R_c \sim 12.5$ k$\Omega \cdot \mu$m for the ion beam-modified Ni-MoS_2, which is a $\sim$50 % reduction compared to the baseline devices. This R_c value is considerably lower than that reported for other Ni-MoS_2, which ranged from 20-30 k$\Omega \cdot \mu$m [26]. While there are other reports of R_c below 1 k$\Omega \cdot \mu$m for different metal-MoS_2 contacts, this is a unique report of substantial reduction in R_c for devices built and compared on the same MoS_2 flake.

There is a trade-off between building single sets of MoS_2 FETs on different flakes/chips where variability in MoS_2 thickness and crystal quality can be high versus two sets of FETs on the same flake to reduce this variation; yet, due to limited flake size, it is challenging to obtain two full sets of devices ($\geq$3 in each set) on the same flake for sufficient TLM data and thus R_c extraction. For this reason, R_c extraction was not possible from most flakes. Also, as can be seen in the Fig. 2(b) output curves, there is evidence of a slight barrier to carrier injection (nonlinearity at low fields) that leads to an overestimation of R_c, which is extracted from the linear low field region. Hence, we focus on the change in I_{on} caused by modifying the contacts, since any differences between devices on the same flake will be strictly occurring at the contacts. In Fig. 2(e), I_{on} change between devices on the same flake with and without ion beam exposure is plotted versus exposure time to statistically determine the impact on FET performance. This shows that the present approach achieves consistent and reproducible enhancement in I_{on} (standard deviation error bars are included) under appropriate ion beam conditions for a large set of different MoS_2 flakes across multiple chips.

Note that another important reason for focusing on I_{on} in comparing the devices rather than R_c is that there are instances where a certain approach for modifying contacts to MoS_2 can dramatically lower R_c but also have deleterious impact on the on-current [20]. The I_{on} comparison for

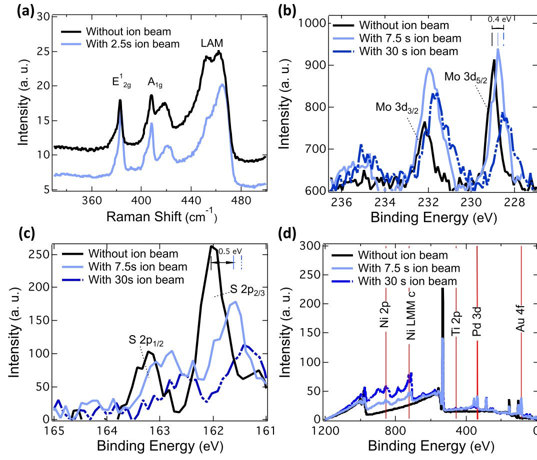

Fig. 3. Characterization of the impact of ion beam exposure on MoS_2. (a) Raman spectroscopy of a MoS_2 flake before and after 2.5 s ion beam exposure. XPS data showing (b) Mo and (c) S peaks from MoS_2 before and after different ion beam exposure times. (d) XPS survey of Si wafers with transferred MoS_2 before and after different ion beam exposure times.

L_{ch} = 200 nm in Fig. 2(e) shows that for exposures longer than ∼14 s, the transistor performance is jeopardized. As expected, there is an optimal exposure time at which the improvement in I_{on} is maximized and this occurs at ∼7 s based on our broad-beam ion source conditions. Note that this type of trade-off between improving carrier injection and causing too much damage to the MoS_2, thus resulting in degradation (exposures of 15 s and above yielding I_{on}(with)/I_{on}(without) <1) of lateral electron transport, has been observed with other contact modification approaches including the etching of graphene [22] and the addition of an insulating layer at the metal-MoS_2 interface [21].

In order to explore how the ion beam is affecting the Ni-MoS_2 interface, Raman spectroscopy (633 nm HeNe Laser) and X-ray photoelectron spectroscopy (XPS) were used to characterize the MoS_2 surface before and after ion beam exposure. The XPS was operated with a monochromatized Al Ka X-ray produced from an anode 15 kW X-ray gun, running with 160 eV pass energy and an emission current of 10 mA. As shown in Fig. 3(a), the change in relative intensity between the E^1_{2g} and A_{1g} peaks of MoS_2 after ion beam exposure of 2.5 s indicates the formation of defects in the lattice. Additionally, the observed right shift of the longitudinal acoustic mode (LAM) is representative of disruption in the MoS_2 lattice after ion beam exposure [27]. This might be explained by the ion beam removing S or Mo in the lattice, where the modified lattice affects the LAM propagating along the MoS_2 plane and hence results in LAM shifts in the 450 cm^{-1} range [27], [28].

Further evidence of defect formation is seen in the XPS spectra of Fig. 3(b-c), where the Mo and S signals are significantly dampened, and in some cases completely attenuated, after ion beam exposure. Note that while the Raman data was obtained from the same MoS_2 flake, the XPS covers an ∼1 mm^2 range across an entire chip of approximately 2 cm × 2 cm, covered with transferred MoS_2 flakes of various thicknesses, ranging from 1 layer to about 50 layers. While it was not possible to deduce the precise nature of the defects, this spectroscopic evidence does support the hypothesis that the ion beam modification creates defects in the MoS_2 lattice that then could promote covalent bonding with the Ni metal contacts. Further extensive characterization is needed to determine the exact bonding profile between Ni and S or Mo. We also note that the *in situ* nature of this ion beam modification process precludes the ability to directly characterize the type of defects formed as the surface has to be exposed to air prior to spectroscopic characterization.

For longer exposure times, the broad peak forming at binding energy ≈235 eV in Fig. 3(b) suggests Mo-O bonding is present for the 7.5 and 30 s ion beam exposures. These Mo-O bonds are attributed to the ion beam-generated defects reacting with O_2 after exposure to air. Also, the Mo $3d_{3/2}$ and $3d_{5/2}$ peaks exhibited right shifting of 0.2 eV and 0.4 eV for 7.5 s and 30 s exposure, respectively. Note that the ratio of Mo $3d_{3/2}$ to $3d_{5/2}$ increases under increasing exposure time; such a ratio change is also present in the transition from MoO_3 to MoS_2 in [29], in which the ratio is decreasing. This is further evidence of how the bonding of Mo changes under different exposure times. Fig. 3(c) demonstrates the right shift of S of 0.5 eV and 0.7 eV after 7.5 s and 30 s ion beam exposure, respectively. Both the Mo and S shifting behavior are congruent with previous reports that use higher energy Ar+ ion beams to modify the basal plane of MoS_2 [30]. Hence, the shift observed in both Mo and S peaks are attributed to the creation of localized defects by the ion beam.

Another important consideration for why the longer ion beam exposure times led to degradation in MoS_2 FET performance is seen in the XPS data of Fig. 3(d). Since we used a broad-beam ion source, the beam spreads throughout the chamber (as illustrated in Fig. 1(e)), leading to sputtering from the chamber sidewalls at longer exposure times. XPS spectra, given in Fig. 3(d), show how a wafer that underwent various exposure times to the ion beam contains a variety of metals, easily identified as Ni, Ti, Pd and Au, which are the metals used in the evaporation system. Though metal peaks can also be seen in the 7.5 s exposure case, it is not as apparent as the chip after 30 s ion beam exposure. Further, sputtered metal from the chamber walls is less clean and leads to the deposition of metal layers that lack homogeneity and thus have uncontrolled and, clearly in this case, unfavorable interfacial behavior. All of these sputtering effects are added complications to the fact that prolonged exposure to the ion beam is also causing excessive damage to the MoS_2.

IV. Conclusion

In conclusion, a new approach to modifying the contact interface between Ni and MoS_2 was presented. Exposing MoS_2 to a broad-beam Ar ion source in UHV introduced defects; in turn, depositing Ni directly onto these defects without breaking vacuum, significantly boosted FET performance. We show R_c reduction on the same MoS_2 flake from 25 kΩ · μm to 12.5 kΩ · μm and a consistent, reproducible enhancement in I_{on} by more than 3× demonstrated in dozens of devices across several chips. These results show a simple and promising approach to engineering contacts to MoS_2 for enhancing performance.

REFERENCES

[1] H. Liu, J. Gu, and P. D. Ye, "MoS_2 nanoribbon transistors: Transition from depletion mode to enhancement mode by channel-width trimming," *IEEE Electron Device Lett.*, vol. 33, no. 9, pp. 1273–1275, Sep. 2012.

[2] A. Dankert, L. Langouche, M. V. Kamalakar, and S. P. Dash, "High-performance molybdenum disulfide field-effect transistors with spin tunnel contacts," *ACS Nano*, vol. 8, no. 1, pp. 476–482, 2014.

[3] S. McDonnell, R. Addou, C. Buie, R. M. Wallace, and C. L. Hinkle, "Defect-dominated doping and contact resistance in MoS_2," *ACS Nano*, vol. 8, no. 3, pp. 2880–2888, Mar. 2014.

[4] S. Kim, A. Konar, W.-S. Hwang, J. H. Lee, J. Lee, J. Yang, C. Jung, H. Kim, J.-B. Yoo, J.-Y. Choi, Y. W. Jin, S. Y. Lee, D. Jena, W. Choi, and K. Kim, "High-mobility and low-power thin-film transistors based on multilayer MoS_2 crystals," *Nature Commun.*, vol. 3, Aug. 2012, Art. no. 1011.

[5] A. D. Franklin, "Nanomaterials in transistors: From high-performance to thin-film applications," *Science*, vol. 349, no. 6249, p. aab2750, 2015.

[6] R. Ganatra and Q. Zhang, "Few-layer MoS_2: A promising layered semiconductor," *ACS Nano*, vol. 8, no. 5, pp. 4074–4099, May 2014.

[7] M. C. Lemme, L.-J. Li, T. Palacios, and F. Schwierz, "Two-dimensional materials for electronic applications," *MRS Bull.*, vol. 39, no. 8, pp. 711–718, Aug. 2014.

[8] A. B. Kaul, "Two-dimensional layered materials: Structure, properties, and prospects for device applications," *J. Mater. Res.*, vol. 29, no. 3, pp. 348–361, Feb. 2014.

[9] K. S. Novoselov, A. K. Geim, S. V. Morozov, D. Jiang, Y. Zhang, S. V. Dubonos, I. V. Grigorieva, and A. A. Firsov, "Electric field effect in atomically thin carbon films," *Science*, vol. 306, no. 5696, pp. 666–669, Oct. 2004.

[10] B. Radisavljevic and A. Kis, "Mobility engineering and a metal–insulator transition in monolayer MoS_2," *Nature Mater.*, vol. 12, no. 9, pp. 815–820, 2013.

[11] W. Bao, X. Cai, D. Kim, K. Sridhara, and M. S. Fuhrer, "High mobility ambipolar MoS_2 field-effect transistors: Substrate and dielectric effects," *Appl. Phys. Lett.*, vol. 102, no. 4, p. 042104, 2013.

[12] B. W. H. Baugher, H. O. H. Churchill, Y. Yang, and P. Jarillo-Herrero, "Intrinsic electronic transport properties of high-quality monolayer and bilayer MoS_2," *Nano Lett.*, vol. 13, no. 9, pp. 4212–4216, 2013.

[13] F. Schwierz, J. Pezoldt, and R. Granzner, "Two-dimensional materials and their prospects in transistor electronics," *Nanoscale*, vol. 7, no. 18, pp. 8261–8283, 2015.

[14] B. Radisavljevic, A. Radenovic, J. Brivio, V. Giacometti, and A. Kis, "Single-layer MoS_2 transistors," *Nature Nanotechnol.*, vol. 6, no. 3, pp. 147–150, Mar. 2011.

[15] Y. Du, H. Liu, A. T. Neal, M. Si, and P. D. Ye, "Molecular doping of multilayer MoS_2 field-effect transistors: Reduction in sheet and contact resistances," *IEEE Electron Device Lett.*, vol. 34, no. 10, pp. 1328–1330, Oct. 2013.

[16] C. D. English, G. Shine, V. E. Dorgan, K. C. Saraswat, and E. Pop, "Improved contacts to MoS_2 transistors by ultra-high vacuum metal deposition," *Nano Lett.*, vol. 16, pp. 3824–3830, 2016.

[17] H.-J. Chuang, B. Chamlagain, M. Koehler, M. M. Perera, J. Yan, D. Mandrus, D. Tománek, and Z. Zhou, "Low-resistance 2D/2D ohmic contacts: A universal approach to high-performance WSe_2, MoS_2, and $MoSe_2$ transistors," *Nano Lett.*, vol. 16, no. 3, pp. 1896–1902, 2016.

[18] J. Kang, W. Liu, and K. Banerjee, "High-performance MoS_2 transistors with low-resistance molybdenum contacts," *Appl. Phys. Lett.*, vol. 104, no. 9, p. 093106, 2014.

[19] S. Das, H.-Y. Chen, A. V. Penumatcha, and J. Appenzeller, "High performance multilayer MoS_2 transistors with scandium contacts," *Nano Lett.*, vol. 13, no. 1, pp. 100–105, 2013.

[20] R. Kappera, D. Voiry, S. E. Yalcin, B. Branch, G. Gupta, A. D. Mohite, and M. Chhowalla, "Phase-engineered low-resistance contacts for ultrathin MoS_2 transistors," *Nature Mater.*, vol. 13, pp. 1–15, Aug. 2014.

[21] S. Lee, A. Tang, S. Aloni, and H.-S. P. Wong, "Statistical study on the Schottky barrier reduction of tunneling contacts to CVD synthesized MoS_2," *Nano Lett.*, vol. 16, no. 1, pp. 276–281, 2015.

[22] J. T. Smith, A. D. Franklin, D. B. Farmer, and C. D. Dimitrakopoulos, "Reducing contact resistance in graphene devices through contact area patterning," *ACS Nano*, vol. 7, no. 4, pp. 3661–3667, 2013.

[23] W. Li, Y. Liang, D. Yu, L. Peng, K. P. Pernstich, T. Shen, A. R. H. Walker, G. Cheng, C. A. Hacker, C. A. Richter, Q. Li, D. J. Gundlach, and X. Liang, "Ultraviolet/ozone treatment to reduce metal-graphene contact resistance," *Appl. Phys. Lett.*, vol. 102, no. 18, p. 183110, 2013.

[24] J. A. Robinson, M. Labella, M. Zhu, M. Hollander, R. Kasarda, Z. Hughes, K. Trumbull, R. Cavalero, and D. Snyder, "Contacting graphene," *Appl. Phys. Lett.*, vol. 98, no. 5, pp. 3–6, 2011.

[25] K. Cho, W. Park, J. Park, H. Jeong, J. Jang, T.-Y. Kim, W.-K. Hong, S. Hong, and T. Lee, "Electric stress-induced threshold voltage instability of multilayer MoS_2 field effect transistors," *ACS Nano*, vol. 7, no. 9, pp. 7751–7758, 2013.

[26] W. S. Leong, X. Luo, Y. Li, K. H. Khoo, S. Y. Quek, and J. T. L. Thong, "Low resistance metal contacts to MoS_2 devices with nickel-etched-graphene electrodes," *ACS Nano*, vol. 9, no. 1, pp. 869–877, 2015.

[27] M. R. Islam, N. Kang, U. Bhanu, H. P. Paudel, M. Erementchouk, L. Tetard, M. N. Leuenberger, and S. I. Khondaker, "Tuning the electrical property via defect engineering of single layer MoS_2 by oxygen plasma," *Nanoscale*, vol. 6, no. 17, pp. 10033–10039, 2014.

[28] R. C. Fivaz and P. Schmid, *Optical and Electronic Properties*. Amsterdam, The Netherlands: Reidel, 1976.

[29] T. Weber, J. C. Muijsers, J. H. M. C. van Wolput, C. P. J. Verhagen, and J. W. Niemantsverdriet, "Basic reaction steps in the sulfidation of crystalline MoO_3 to MoS_2, as studied by X-ray photoelectron and infrared emission spectroscopy," *J. Phys. Chem.*, vol. 100, no. 33, pp. 14144–14150, 1996.

[30] N. S. McIntyre, P. A. Spevack, G. Beamson, and D. Briggs, "Effects of argon ion bombardment on basal plane and polycrystalline MoS_2," *Surf. Sci.*, vol. 237, nos. 1–3, pp. L390–L397, 1990.